# Time-domain implementation of the optimal cross-correlation statistic for stochastic gravitational-wave background searches in pulsar timing data

Sydney J. Chamberlin,[*] Jolien D. E. Creighton,[†] and Xavier Siemens[‡]
*Center for Gravitation, Cosmology, and Astrophysics, Department of Physics, University of Wisconsin–Milwaukee, Milwaukee, Wisconsin 53201, USA*

Paul Demorest[§]
*National Radio Astronomy Observatory, Charlottesville, Virginia 22903 USA*

Justin Ellis[¶,**]
*Jet Propulsion Laboratory, California Institute of Technology, Pasadena, California 91109, USA*

Larry R. Price[††]
*LIGO Laboratory, California Institute of Technology, Pasadena, California 91125, USA*

Joseph D. Romano[‡‡]
*Department of Physics and Astronomy and Center for Gravitational-Wave Astronomy, University of Texas at Brownsville, Brownsville, Texas 78520, USA*
(Received 30 October 2014; published 27 February 2015)

Supermassive black hole binaries, cosmic strings, relic gravitational waves from inflation, and first-order phase transitions in the early Universe are expected to contribute to a stochastic background of gravitational waves in the $10^{-9}$–$10^{-7}$ Hz frequency band. Pulsar timing arrays (PTAs) exploit the high-precision timing of radio pulsars to detect signals at such frequencies. Here we present a time-domain implementation of the optimal cross-correlation statistic for stochastic background searches in PTA data. Due to the irregular sampling typical of PTA data as well as the use of a timing model to predict the times of arrival of radio pulses, time-domain methods are better-suited for gravitational-wave data analysis of such data. We present a derivation of the optimal cross-correlation statistic starting from the likelihood function, a method to produce simulated stochastic background signals, and a rigorous derivation of the scaling laws for the signal-to-noise ratio of the cross-correlation statistic in the two relevant PTA regimes: the weak-signal limit where instrumental noise dominates over the gravitational-wave signal at all frequencies, and a second regime where the gravitational-wave signal dominates at the lowest frequencies.

DOI: 10.1103/PhysRevD.91.044048 PACS numbers: 04.30.-w, 04.80.Nn

## I. INTRODUCTION

Gravitational waves, a key prediction of Einstein's theory of general relativity, are perturbations in the fabric of spacetime produced by the accelerated motion of massive objects. The direct detection of gravitational waves is likely to occur in the next few years, and promises to provide a new means to study the Universe. A number of worldwide efforts aiming to detect gravitational waves are currently under way. At the low-frequency end of the detectable gravitational-wave spectrum ($10^{-9}$–$10^{-7}$ Hz), pulsar timing arrays (PTAs) exploit the remarkable high-precision timing of radio pulsars to search for gravitational waves [1]. Pulsars have already been used to indirectly measure the effects of gravitational-wave emission through the Hulse-Taylor binary [2]. A direct detection of gravitational waves is possible with an array of precisely timed pulsars: a gravitational wave propagating through spacetime affects the travel time of radio pulses from pulsars, and can be observed by searching for correlated deviations in the expected times of arrival of the radio pulses [3,4].

The most likely source of gravitational waves at nanohertz frequencies are supermassive black hole binaries (SMBBHs) that form following the merger of massive galaxies [5–7]. The superposition of gravitational waves from all SMBBH mergers forms a stochastic background of gravitational waves [5,6,8–13]. Individual periodic signals [7,14–17] and bursts [18,19] can also be produced by SMBBH systems. In addition, cosmic strings [20–23], first-order phase transitions in the early Universe [24], and relic gravitational waves from inflation [25,26] are potential sources of gravitational waves in the nanohertz band.

[*]sydc@gravity.phys.uwm.edu
[†]jolien@gravity.phys.uwm.edu
[‡]siemens@gravity.phys.uwm.edu
[§]pdemores@nrao.edu
[¶]Justin.A.Ellis@jpl.nasa.gov
[**]Einstein Fellow
[††]larryp@caltech.edu
[‡‡]joe@phys.utb.edu

 

A number of data analysis techniques have been developed and implemented to search for isotropic stochastic backgrounds of gravitational waves in PTA data [4,16,27–40]. More recently, these techniques have been generalized to searches for anisotropic backgrounds [41–44]. Additionally, a range of data analysis methods have been developed to search for individual periodic sources that stand out over the stochastic background [7,14,15,17,45–53], bursts [54–58], and signals of unknown form [59].

In this paper we describe a practical time-domain implementation of the optimal cross-correlation statistic [31] that can be used to search for isotropic stochastic backgrounds. In Sec. II, we review the effect of a gravitational wave on the pulsar-Earth system, and the expected cross-correlations in the times of arrival of pulses from different pulsars. In Sec. III, we develop the formalism needed to implement the search for a stochastic background, including the timing model, and derive the optimal cross-correlation statistic from the likelihood ratio. In Sec. IV, we develop a procedure for injecting simulated stochastic background signals into PTA data, and in Sec. V, we describe the scaling laws that govern the expected signal-to-noise ratio of the cross-correlation statistic. We conclude in Sec. VI with a discussion of the practicality of implementing the statistics introduced in this paper for gravitational-wave searches. For reference, we will work in units where $c = G = 1$.

## II. PRELIMINARIES

An array of pulsars can be used to search for a stochastic background of gravitational waves. Deviations from the expected times of arrival of pulses from different pulsars are correlated, and with enough timing precision these correlations are measurable. In this section we describe how the times of arrival of pulses from pulsars are affected by gravitational waves, and discuss the expected correlation of signals from different pulsars.

Gravitational waves induce a redshift in the signal from the pulsar that depends on the geometry of the pulsar-Earth system and the metric perturbation [4]. For a pulsar located in the direction of unit vector $\hat{p}$ (that points from Earth to the pulsar), and a gravitational wave propagating in the direction $\hat{\Omega}$ (see Fig. 1), the redshift induced in the radio pulse is proportional to the change in the metric perturbation at the Earth, when the pulse is received, and at the pulsar, when the pulse is emitted [4,31]

$$z(t,\hat{\Omega}) = \frac{1}{2}\frac{\hat{p}^i\hat{p}^j}{1+\hat{\Omega}\cdot\hat{p}}\Delta h_{ij}, \tag{1}$$

where[1]

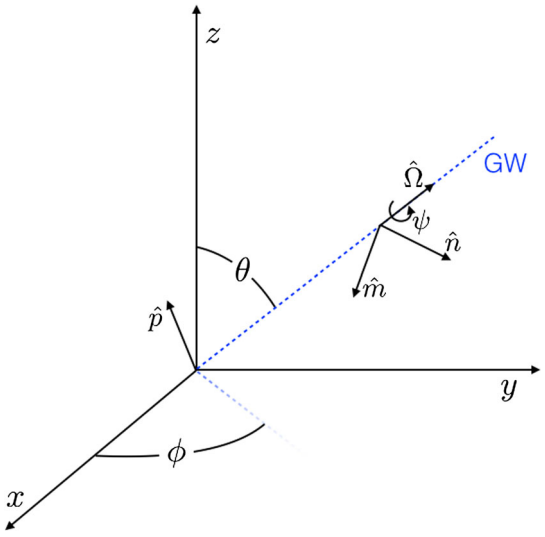


FIG. 1 (color online). The pulsar-Earth system, as visualized with the Earth at the origin. The gravitational wave propagates as the blue dashed line, and the vectors defined in Eqs. (8a)–(8c) are included with polar and azimuthal angles. The angle $\psi$ designates the polarization angle of the gravitational wave. For a stochastic gravitational-wave background, this angle is averaged over many independent sources and can be chosen to be zero.

$$\Delta h_{ij} \equiv h_{ij}(t_e,\hat{\Omega}) - h_{ij}(t_p,\hat{\Omega}) \tag{2}$$

and $i, j$ denote spatial components.[2] These terms are typically referred to as the Earth term and the pulsar term, respectively.

The total redshift is obtained by integrating Eq. (1) over all directions on the sky

$$z(t) = \int_{S^2} d\hat{\Omega} z(t,\hat{\Omega}). \tag{3}$$

It is important to point out that in pulsar timing the observable quantity is actually not the redshift, but the *timing residual*, which is just the integral of the redshift

$$r(t) = \int_0^t dt' z(t'). \tag{4}$$

The metric perturbation in terms of the usual plane wave expansion is [60]

$$h_{ij}(t,\vec{x}) = \sum_A \int_{-\infty}^{\infty} df \int_{S^2} d\hat{\Omega} e^{i2\pi f(t-\hat{\Omega}\cdot\vec{x})} h_A(f,\hat{\Omega}) e^A_{ij}(\hat{\Omega}), \tag{5}$$

where $f$ is the frequency of the gravitational wave, $A = +,\times$ labels the polarization modes, and $e^A_{ij}(\hat{\Omega})$ are

[1]Here we correct a sign error in a previous paper [31], pointed out to us by Eanna Flanagan.

[2]Note that in this section we use the Einstein summation notation where repeated indices are summed over.

the polarization tensors (see below). We can use this expansion to write a frequency-domain expression for the timing residuals produced by a gravitational wave traveling in the direction $\hat{\Omega}$. Specifically,

$$\tilde{r}(f,\hat{\Omega}) = \frac{1}{2\pi i f}(1 - e^{-2\pi i f L(1+\hat{\Omega}\cdot\hat{p})}) \times \sum_A h_A(f,\hat{\Omega})\left(e^A_{ij}(\hat{\Omega})\frac{\hat{p}^i\hat{p}^j}{2(1+\hat{\Omega}\cdot\hat{p})}\right), \quad (6)$$

where $L$ is the pulsar-Earth distance.

The polarization tensors are

$$e^+_{ij}(\hat{\Omega}) = \hat{m}_i\hat{m}_j - \hat{n}_i\hat{n}_j, \quad (7a)$$

$$e^\times_{ij}(\hat{\Omega}) = \hat{m}_i\hat{n}_j + \hat{n}_i\hat{m}_j, \quad (7b)$$

where the quantities

$$\hat{\Omega} = (\sin\theta\cos\phi, \sin\theta\sin\phi, \cos\theta) = \hat{r}, \quad (8a)$$

$$\hat{m} = (\sin\phi, -\cos\phi, 0) = -\hat{\phi}, \quad (8b)$$

$$\hat{n} = (\cos\theta\cos\phi, \cos\theta\sin\phi, -\sin\theta) = \hat{\theta} \quad (8c)$$

describe the geometry of the propagating gravitational wave as shown in Fig. 1.

The energy density of gravitational waves is given by

$$\rho_{\rm gw} = \frac{1}{32\pi}\langle \dot{h}_{ij}(t,\vec{x})\dot{h}^{ij}(t,\vec{x})\rangle, \quad (9)$$

and the spectrum of a stochastic background is

$$\Omega_{\rm gw}(f) \equiv \frac{1}{\rho_{\rm crit}}\frac{d\rho_{\rm gw}}{d\ln f}, \quad (10)$$

where $\rho_{\rm crit} = 3H_0^2/(8\pi)$ is the critical energy density, and $H_0$ is the Hubble constant.

The stochastic background produces changes in the timing residuals of individual pulsars that are correlated between different pulsars. As Hellings and Downs showed [61], the cross-correlation of the timing residuals from two pulsars $I$ and $J$ depends only on the angular separation $\zeta_{IJ}$ of the two pulsars:

$$\langle \tilde{r}^*_I(f)\tilde{r}_J(f')\rangle = \frac{H_0^2}{16\pi^4}\delta(f-f')|f|^{-5}\Omega_{\rm gw}(|f|)\chi_{IJ}, \quad (11)$$

where

$$\chi_{IJ} = \frac{3}{2}\left[\frac{1}{3} + \frac{1-\cos\zeta_{IJ}}{2}\left[\ln\left(\frac{1-\cos\zeta_{IJ}}{2}\right) - \frac{1}{6}\right]\right] + \frac{1}{2}\delta_{IJ}. \quad (12)$$

This follows from Eq. (6) for the timing residuals in the frequency domain, assuming

$$\langle h^*_A(f,\hat{\Omega})h_{A'}(f',\hat{\Omega}')\rangle = \frac{3H_0^2}{32\pi^3}\delta^2(\hat{\Omega},\hat{\Omega}')\delta_{AA'}\delta(f-f') \times |f|^{-3}\Omega_{\rm gw}(|f|) \quad (13)$$

for an isotropic, unpolarized, and stationary stochastic background [31,60]. The pulsar term in Eq. (6), proportional to $e^{-2\pi i f L(1+\hat{\Omega}\cdot\hat{p})}$, contributes to the expectation value in Eq. (11) only when we are dealing with the same pulsar (i.e., when $I = J$), and averages to zero for different pulsars [31].

In parts of this paper, we will refer not to $\Omega_{\rm gw}(f)$ but instead to the dimensionless gravitational-wave amplitude $A_{\rm gw}$ (at reference frequency $f_{1\ \rm yr} = \rm yr^{-1}$) which appears in the expression for the characteristic strain

$$h_c(f) = A_{\rm gw}\left(\frac{f}{f_{1\ \rm yr}}\right)^\alpha. \quad (14)$$

The spectral index $\alpha$ depends on the astrophysical source of the background. For example, a stochastic background produced by supermassive black hole binary systems has $\alpha = -2/3$ [5,6]. The amplitude $A_{\rm gw}$ is related to the strain spectral density $S_h(f)$ of the gravitational-wave background via

$$S_h(f) = \frac{h_c^2(f)}{f}. \quad (15)$$

For one-sided power spectra, $S_h(f)$ and $A_{\rm gw}$ are related to $\Omega_{\rm gw}(f)$ by

$$S_h(f) = \frac{3H_0^2}{2\pi^2}\frac{\Omega_{\rm gw}(f)}{f^3}, \quad (16)$$

$$\Omega_{\rm gw}(f) = \frac{2\pi^2}{3H_0^2}A_{\rm gw}^2 f^2\left(\frac{f}{f_{1\ \rm yr}}\right)^{2\alpha}. \quad (17)$$

Note that in this paper we will work exclusively with one-sided spectra, which differs from the convention adopted in [62].

## III. THE OPTIMAL CROSS-CORRELATION STATISTIC

### A. Timing model

In pulsar timing experiments the quantities that are directly measured are the times of arrival (TOAs) of radio pulses emitted from pulsars. These TOAs contain many terms of known functional form, including intrinsic pulsar parameters (pulsar period, spin-down, etc.), along with stochastic processes such as radiometer noise, pulse phase jitter, and possibly red noise either from interstellar medium

(ISM) effects, intrinsic pulsar noise, and, potentially, a gravitational-wave background.

Suppose that the TOAs for a pulsar are given by

$$\mathbf{t}^{\rm obs} = \mathbf{t}^{\rm det}(\boldsymbol{\xi}_{\rm true}) + \mathbf{n}, \tag{18}$$

where $\mathbf{t}^{\rm obs}$ are the $N_{\rm TOA}$ observed TOAs, $\mathbf{t}^{\rm det}$ are the deterministic modeled TOAs parametrized by $N_{\rm par}$ timing model parameters $\boldsymbol{\xi}_{\rm true}$, and $\mathbf{n}$ is the noise time series in the measurement which is assumed to be Gaussian with covariance matrix given by

$$\mathbf{N} = \langle \mathbf{n}\mathbf{n}^T \rangle = \mathbf{N}^{\rm white} + \mathbf{N}^{\rm red} \tag{19}$$

where the $N_{\rm TOA} \times N_{\rm TOA}$ matrices $\mathbf{N}^{\rm white}$ and $\mathbf{N}^{\rm red}$ are the contributions to the covariance matrix from the white and red noise processes, respectively. We will discuss the exact form of this covariance matrix in the next section. Assuming that estimates of the true timing model parameters $\boldsymbol{\xi}_{\rm est}$ exist (either from information gained when discovering the pulsar or from past timing observations), we can form the prefit timing residuals as

$$\delta\mathbf{t}^{\rm pre} = \mathbf{t}^{\rm obs} - \mathbf{t}^{\rm det}(\boldsymbol{\xi}_{\rm est}) = \mathbf{t}^{\rm det}(\boldsymbol{\xi}_{\rm true}) + \mathbf{n} - \mathbf{t}^{\rm det}(\boldsymbol{\xi}_{\rm est}). \tag{20}$$

As mentioned above, we will assume that the initial estimates for our timing model parameters are correct to some linear offset $\boldsymbol{\xi}_{\rm est} = \boldsymbol{\xi}_{\rm true} + \delta\boldsymbol{\xi}$, for which the prefit residuals become

$$\delta\mathbf{t}^{\rm pre} = \mathbf{t}^{\rm det}(\boldsymbol{\xi}_{\rm true}) - \mathbf{t}^{\rm det}(\boldsymbol{\xi}_{\rm true} + \delta\boldsymbol{\xi}) + \mathbf{n}. \tag{21}$$

Expanding this solution around the true timing model parameters, we obtain

$$\begin{aligned}\delta\mathbf{t}^{\rm pre} &= -\left.\frac{\partial \mathbf{t}^{\rm det}}{\partial \boldsymbol{\xi}}\right|_{\boldsymbol{\xi}=\boldsymbol{\xi}_{\rm true}} \delta\boldsymbol{\xi} + \mathbf{n} + \mathcal{O}(\delta\boldsymbol{\xi}^2) \\ &\approx -\left.\frac{\partial \mathbf{t}^{\rm det}}{\partial \boldsymbol{\xi}}\right|_{\boldsymbol{\xi}=\boldsymbol{\xi}_{\rm true}} \delta\boldsymbol{\xi} + \mathbf{n} \\ &= \mathbf{M}\delta\boldsymbol{\xi} + \mathbf{n},\end{aligned} \tag{22}$$

where $\mathbf{M}$ is an $N_{\rm TOA} \times N_{\rm par}$ matrix, commonly referred to as the *design matrix* [63,64]. Here we have assumed that our initial estimate of the model parameters is sufficiently close to the true values so that we can approximate this as a linear system of equations in $\delta\boldsymbol{\xi}$. It is customary in standard pulsar timing analysis to obtain the best fit $\delta\boldsymbol{\xi}$ values through a generalized least-squares minimization of the prefit residuals. The function that we seek to minimize is (see [65])

$$\chi^2 = \frac{1}{2}(\delta\mathbf{t}^{\rm pre} - \mathbf{M}\delta\boldsymbol{\xi})^T\mathbf{N}^{-1}(\delta\mathbf{t}^{\rm pre} - \mathbf{M}\delta\boldsymbol{\xi}). \tag{23}$$

Minimizing this function with respect to the parameter offsets $\delta\boldsymbol{\xi}$ results in

$$\delta\boldsymbol{\xi}_{\rm best} = -(\mathbf{M}^T\mathbf{N}^{-1}\mathbf{M})^{-1}\mathbf{M}^T N^{-1}\delta\mathbf{t}^{\rm pre}. \tag{24}$$

The postfit residuals are then given by

$$\delta\mathbf{t}^{\rm post} \equiv \delta\mathbf{t}^{\rm pre} - \mathbf{M}\delta\boldsymbol{\xi}_{\rm best} = \mathbf{R}\delta\mathbf{t}^{\rm pre}, \tag{25}$$

where

$$\mathbf{R} = \mathbb{I} - \mathbf{M}(\mathbf{M}^T\mathbf{N}^{-1}\mathbf{M})^{-1}\mathbf{M}^T\mathbf{N}^{-1} \tag{26}$$

is an $N_{\rm TOA} \times N_{\rm TOA}$ oblique projection matrix that transforms prefit to postfit residuals, and $\mathbb{I}$ is the identity matrix. All of the information about any noise source or stochastic gravitational-wave background is encoded in $\mathbf{N}$. However, in most cases we have no *a priori* knowledge of this covariance matrix and therefore assume that it is given by $\mathbf{W} = \mathrm{diag}(\{\sigma_i^2\})$, where $\sigma_i$ is the uncertainty of the $i$th TOA. Previous work [66] has used an iterative method to estimate the covariance matrix of the residuals and apply a generalized least-squares fit. For this work we will only work with residuals that have been created using a weighted least-squares fit. It should be noted that in standard pulsar timing packages such as TEMPO2 [65] this process must be iterated. In other words, the prefit residuals are formed with an initial guess of the parameters, and the chi squared is then minimized to produce best estimates of the parameters. This may not be a good fit, however, as we have assumed that the prefit residuals are linear in the parameter offsets. Consequently, we form new parameter estimates from the best fit parameter offsets and iterate until the fit converges, with the reduced chi squared serving as the goodness-of-fit parameter. For this reason, we must ensure that our timing model fit has converged prior to any gravitational-wave analysis.

### B. Derivation of the optimal statistic

#### 1. Likelihood function for a PTA

Much of the discussion in this section follows closely that of [40], with some of the details included here. We begin by assuming that our PTA consists of $M$ pulsars, each with some intrinsic noise $\mathbf{n}_I(t)$. Henceforth uppercase latin indices will label a pulsar and lowercase latin indices will label a particular TOA. Under the assumption that all intrinsic pulsar noise is Gaussian, we can write the full likelihood function for the PTA as

$$p(\mathbf{n}|\vec{\theta}) = \frac{1}{\sqrt{\det(2\pi\Sigma_n)}}\exp\left(-\frac{1}{2}\mathbf{n}^T\Sigma_n^{-1}\mathbf{n}\right), \tag{27}$$

where now we are using the full PTA noise time series that is just a concatenated length $MN_{\rm TOA}$ column vector

$$\mathbf{n} = \begin{bmatrix} \mathbf{n}_1 \\ \mathbf{n}_2 \\ \vdots \\ \mathbf{n}_M \end{bmatrix}, \tag{28}$$

$\Sigma_n$ is the $MN_{\rm TOA} \times MN_{\rm TOA}$ covariance matrix, and $\vec{\theta}$ is a set of parameters that characterize the noise. The covariance matrix for the noise is the block matrix

$$\Sigma_n = \begin{bmatrix} \mathbf{N}_1 & \mathbf{X}_{12} & \cdots & \mathbf{X}_{1M} \\ \mathbf{X}_{12} & \mathbf{N}_2 & \cdots & \mathbf{X}_{2M} \\ \vdots & \vdots & \ddots & \vdots \\ \mathbf{X}_{M1} & \mathbf{X}_{M2} & \ldots & \mathbf{N}_M \end{bmatrix}, \tag{29}$$

where

$$\mathbf{N}_I = \langle \mathbf{n}_I \mathbf{n}_I^T \rangle, \tag{30}$$

$$\mathbf{X}_{IJ} = \langle \mathbf{n}_I \mathbf{n}_J^T \rangle|_{I \neq J}, \tag{31}$$

are the autocovariance and cross-covariance matrices, respectively, for each set of noise vectors.

In general the autocorrelation matrices are defined via the Wiener-Khinchin theorem as

$$\mathbf{N}_I = \langle \mathbf{n}_I \mathbf{n}_I^T \rangle_{ij} = \int_0^\infty df e^{2\pi i f \tau_{ij}} \mathcal{P}_I(f) + \mathcal{F}_I \mathbf{W}_I + \mathcal{Q}_I^2 \mathbb{I} \tag{32}$$

where $\tau_{ij} = |t_i - t_j|$, $\mathcal{F}_I$ and $\mathcal{Q}_I$ are white-noise parameters for pulsar $I$ (usually denoted as EFAC and EQUAD, respectively), $\mathbb{I}$ is the identity matrix, and $\mathcal{P}_I(f)$ is a red-noise power spectrum

$$\mathcal{P}_I(f) = \mathcal{P}_I^{\rm int}(f) + \mathcal{P}_g(f) \tag{33}$$

where

$$\mathcal{P}_I^{\rm int}(f) = \frac{A_I^2}{12\pi^2} \left( \frac{f}{f_{1\ \rm yr}} \right)^{2\alpha_I} f^{-3} \tag{34}$$

is the intrinsic red noise in the pulsar parametrized by amplitude $A_I$ and spectral index $\alpha_I$, and

$$\mathcal{P}_g(f) = \frac{A_{\rm gw}^2}{12\pi^2} \left( \frac{f}{f_{1\ \rm yr}} \right)^{2\alpha} f^{-3} \tag{35}$$

is the gravitational-wave background spectrum parametrized by the strain amplitude $A_{\rm gw}$ and spectral index $\alpha$. In other words, the autocovariance matrix of the noise in pulsar $I$ consists of intrinsic white noise parametrized by $\{\mathcal{F}_I, \mathcal{Q}_I\}$ and red noise parametrized by $\{A_I, \alpha_I, A_{\rm gw}, \gamma\}$. Notice that the gravitational-wave parameters do not have a pulsar label because they are common to all pulsars.

Similarly, the cross-covariance matrices are given by

$$X_{IJ} = \langle \mathbf{n}_I \mathbf{n}_J^T \rangle_{ij} = \chi_{IJ} \int_0^\infty df e^{2\pi i f \tau_{ij}} \mathcal{P}_g(f) \tag{36}$$

where $\chi_{IJ}$ are the Hellings and Downs coefficients for pulsar pair $I, J$ defined in Eq. (12).

We now write the likelihood function for the timing residuals using Eqs. (22) and (27) as

$$p(\delta\mathbf{t}|\vec{\theta}, \delta\boldsymbol{\xi}) = \frac{\exp\left(-\frac{1}{2}(\delta\mathbf{t} - \mathbf{M}\delta\boldsymbol{\xi})^T \Sigma_n^{-1} (\delta\mathbf{t} - \mathbf{M}\delta\boldsymbol{\xi})\right)}{\sqrt{\det(2\pi\Sigma_n)}}, \tag{37}$$

where $\delta\mathbf{t}$ and $\delta\boldsymbol{\xi}$ are defined in an identical manner as $\mathbf{n}$ as the concatenated vector or residuals and timing parameters for each pulsar, respectively. Note that here we use $\delta\mathbf{t}$ instead of $\delta\mathbf{t}^{\rm pre}$ since this process can be thought of as another step in the iterative process of timing (where the postfit residuals are formed from the previous set of prefit residuals); instead of minimizing the chi squared using $\mathbf{W}$ as the noise covariance, we now use the full noise covariance matrix $\Sigma_n$ and the full PTA data set to *maximize* the likelihood. In [39] it was shown that this likelihood can be maximized[3] analytically over the timing model parameters to give

$$p(\delta\mathbf{t}|\vec{\theta}) = \frac{\exp\left(-\frac{1}{2}\delta\mathbf{t}^T \mathbf{G}(\mathbf{G}^T\Sigma_n\mathbf{G})^{-1}\mathbf{G}^T\delta\mathbf{t}\right)}{\sqrt{\det(2\pi\Sigma_n)}}, \tag{38}$$

where $\mathbf{G}_I$ is an $N_{\rm TOA} \times (N_{\rm TOA} - N_{\rm par})$ matrix. The matrix $\mathbf{G}_I^T$ spans the null space of $\mathbf{M}_I$ and will project the data onto a subspace orthogonal to the linearized timing model. The full PTA G matrix is then

$$\mathbf{G} = \begin{bmatrix} \mathbf{G}_1 & 0 & \cdots & 0 \\ 0 & \mathbf{G}_2 & \cdots & 0 \\ \vdots & \vdots & \ddots & \vdots \\ 0 & 0 & \cdots & \mathbf{G}_M \end{bmatrix}. \tag{39}$$

For the remainder of paper we will use the following notation

$$\mathbf{r}_I = \mathbf{G}_I^T \delta\mathbf{t}_I, \tag{40}$$

[3]In [39], the authors actually *marginalize* the likelihood function over the pulsar timing parameters; however, when using uniform priors the resulting likelihood after maximizing or marginalizing only differs by a factor of $\det(\mathbf{M}^T\Sigma_n\mathbf{M})$, so the data-dependent part of the likelihood remains the same.

$$\mathbf{P}_I = \mathbf{G}_I^T \mathbf{N}_I \mathbf{G}_I, \tag{41}$$

$$\mathbf{S}_{IJ} = \mathbf{G}_I^T \mathbf{X}_{IJ} \mathbf{G}_J, \tag{42}$$

$$\Sigma = \mathbf{G}^T \Sigma_n \mathbf{G}, \tag{43}$$

with the likelihood function written as

$$p(\mathbf{r}|\vec{\theta}) = \frac{1}{\sqrt{\det(2\pi\Sigma_n)}} \exp\left(-\frac{1}{2}\mathbf{r}^T\Sigma^{-1}\mathbf{r}\right). \tag{44}$$

### 2. Time-domain optimal statistic

In [31] some of us presented the optimal cross-correlation statistic in both the frequency and time domains, with a focus on the frequency-domain implementation. The nonstationarity that arises from the timing model fit [Eq. (26)], along with the irregular sampling that is typical of realistic PTA data sets, however, make frequency-domain techniques unsuitable for PTA gravitational-wave data analysis. Therefore in this paper we will focus on the time-domain implementation of the cross-correlation statistic. In [31] the time-domain derivation was done by constructing the likelihood ratio of a model that contained a stochastic gravitational-wave background and intrinsic noise to a model that contained only intrinsic noise. It was assumed that the amplitude of the intrinsic noise is much larger than the amplitude of the gravitational-wave background, and thus can be safely ignored in the autocovariance matrices of the residuals. One can then perform an expansion of the log-likelihood ratio in powers of a small order parameter taken to represent the amplitude of the background. This assumption can lead to a significant bias in the recovered amplitude of the gravitational-wave background if the background is sufficiently large.

Fortunately it is possible to carry out a nearly identical derivation that takes into account a potential non-negligible contribution of the stochastic background to the autocovariance terms. In [40] it was shown that it is possible to expand the covariance matrix $\Sigma$ in a Taylor series expansion in the Hellings and Downs coefficients (as opposed to an expansion in the amplitude of the background) to obtain a "first-order" likelihood function. The log of this likelihood function can be written as

$$\ln p(\mathbf{r}|\vec{\theta}) \approx -\frac{1}{2}\left[\sum_{I=1}^{M}(\mathrm{tr}\ln\mathbf{P}_I + \mathbf{r}_I^T\mathbf{P}_I^{-1}\mathbf{r}_I) - \sum_{IJ}\mathbf{r}_I^T\mathbf{P}_I^{-1}\mathbf{S}_{IJ}\mathbf{P}_J^{-1}\mathbf{r}_J\right] \tag{45}$$

where $\sum_{IJ} = \sum_{I=1}^{M}\sum_{J<I}^{M}$ is a sum over all *unique* pulsar pairs. Let us now assume that we have done a single pulsar noise analysis [39,67] on each pulsar so that we know $\mathbf{P}_I$, and consider the following log-likelihood ratio

$$\ln\Lambda = \ln p(\mathbf{r}|\vec{\theta}_{\mathrm{gw}}) - \ln p(\mathbf{r}|\vec{\theta}_{\mathrm{noise}}). \tag{46}$$

Here $\vec{\theta}_{\mathrm{gw}}$ are the parameters for a model with a *spatially correlated*[4] gravitational-wave background component along with uncorrelated red- and white-noise components, which include the gravitational-wave background present in the pulsar term, ISM noise, radiometer noise, jitter noise, etc. The parameters $\vec{\theta}_{\mathrm{noise}}$ are for a model with only *spatially uncorrelated* noise components. We treat the autocovariance of each pulsar as a known measured quantity of the PTA data after the aforementioned noise analysis has been done. In this case, if we fix the spectral index to, say, the one corresponding to SMBBH backgrounds with a spectral index $\alpha = -2/3$, the only free parameter is the amplitude of the gravitational-wave background. Evaluating this log-likelihood ratio we have

$$\ln\Lambda = \frac{A_{\mathrm{gw}}^2}{2}\sum_{IJ}\mathbf{r}_I^T\mathbf{P}_J^{-1}\tilde{\mathbf{S}}_{IJ}\mathbf{P}_J^{-1}\mathbf{r}_J, \tag{47}$$

where we have used the amplitude-independent cross-correlation matrix $\tilde{\mathbf{S}}_{IJ}$ defined by

$$A_{\mathrm{gw}}^2\tilde{\mathbf{S}}_{IJ} = \langle\mathbf{r}_I\mathbf{r}_J^T\rangle = \mathbf{S}_{IJ}. \tag{48}$$

Notice that all terms that only include the autocovariance matrices are canceled by the noise model likelihood function. Note also that this expression is nearly identical to Eq. (75) of [31] with the caveat that now we are dealing exclusively with postfit quantities and have allowed for a non-negligible contribution from the gravitational-wave background in the autocovariance matrices. From Eq. (47) we define the optimal cross-correlation statistic for a PTA to be

$$\hat{A}^2 = \frac{\sum_{IJ}\mathbf{r}_I^T\mathbf{P}_I^{-1}\tilde{\mathbf{S}}_{IJ}\mathbf{P}_J^{-1}\mathbf{r}_J}{\sum_{IJ}\mathrm{tr}[\mathbf{P}_I^{-1}\tilde{\mathbf{S}}_{IJ}\mathbf{P}_J^{-1}\tilde{\mathbf{S}}_{JI}]}, \tag{49}$$

where the normalization factor

$$\mathcal{N} \equiv \left(\sum_{IJ}\mathrm{tr}[\mathbf{P}_I^{-1}\tilde{\mathbf{S}}_{IJ}\mathbf{P}_J^{-1}\tilde{\mathbf{S}}_{JI}]\right)^{-1} \tag{50}$$

is chosen so that on average $\langle\hat{A}^2\rangle = A_{\mathrm{gw}}^2$. This immediately follows from the observation that

$$\left\langle\sum_{IJ}\mathbf{r}_I^T\mathbf{P}_I^{-1}\tilde{\mathbf{S}}_{IJ}\mathbf{P}_J^{-1}\mathbf{r}_J\right\rangle = \sum_{IJ}\mathrm{tr}[\mathbf{P}_I^{-1}\tilde{\mathbf{S}}_{IJ}\mathbf{P}_J^{-1}\mathbf{S}_{JI}] = A_{\mathrm{gw}}^2\sum_{IJ}\mathrm{tr}[\mathbf{P}_I^{-1}\tilde{\mathbf{S}}_{IJ}\mathbf{P}_J^{-1}\tilde{\mathbf{S}}_{JI}], \tag{51}$$

where Eq. (48) was used in the second line.

[4]By spatially correlated we mean that the correlation is parametrized by the Hellings and Downs curve.

In the absence of a cross-correlated signal (or if the signal is weak) the expectation value of $\hat{A}^2$ vanishes and its standard deviation is [31]

$$\sigma_0 = \left(\sum_{IJ} \mathrm{tr}[\mathbf{P}_I^{-1}\tilde{\mathbf{S}}_{IJ}\mathbf{P}_J^{-1}\tilde{\mathbf{S}}_{JI}]\right)^{-1/2}, \tag{52}$$

so if in a particular realization we measure a value of the optimal statistic, the signal-to-noise ratio (SNR) for the *power in the cross-correlations* for that realization is

$$\hat{\rho} = \frac{\hat{A}^2}{\sigma_0} = \frac{\sum_{IJ}\mathbf{r}_I^T\mathbf{P}_I^{-1}\tilde{\mathbf{S}}_{IJ}\mathbf{P}_J^{-1}\mathbf{r}_J}{(\sum_{IJ}\mathrm{tr}[\mathbf{P}_I^{-1}\tilde{\mathbf{S}}_{IJ}\mathbf{P}_J^{-1}\tilde{\mathbf{S}}_{JI}])^{1/2}} \tag{53}$$

with an expectation value over all realizations of

$$\langle\rho\rangle = A_{\mathrm{gw}}^2\left(\sum_{IJ}\mathrm{tr}[\mathbf{P}_I^{-1}\tilde{\mathbf{S}}_{IJ}\mathbf{P}_J^{-1}\tilde{\mathbf{S}}_{JI}]\right)^{1/2}. \tag{54}$$

Note that this definition of the SNR measures the confidence (in standard deviations) with which we can reject the null hypothesis that there are no *spatially correlated* signals in our data. To clarify this a bit further we outline a standard frequentist hypothesis detection procedure:

(1) Measure the optimal statistic value, $\hat{A}^2$ of Eq. (49), for our data set.
(2) Compute the probability $p(\hat{A}^2 > \hat{A}^2_{\mathrm{thresh}}|A_{\mathrm{gw}} = 0)$, that is, the probability that our measurement of the optimal statistic $\hat{A}^2$ is greater than some threshold value of the statistic $\hat{A}^2_{\mathrm{thresh}}$ assuming that the null hypothesis $A_{\mathrm{gw}} = 0$ is true.
(3) If the aforementioned probability (sometimes called the $p$ value) is less than some value [this value is set to be a tolerable yet problem-specific false-alarm probability (FAP)] then a detection is claimed.

Typically $\hat{A}^2_{\mathrm{thresh}}$ is given by

$$\alpha = \int_{-\infty}^{\hat{A}^2_{\mathrm{thresh}}} d\hat{A}^2 p(\hat{A}^2|A_{\mathrm{gw}} = 0), \tag{55}$$

where $\alpha = 1 - \mathrm{FAP}$ and $p(\hat{A}^2|A_{\mathrm{gw}} = 0)$ is the probability distribution function of the optimal statistic given the null hypothesis. To a sufficiently good approximation, $p(\hat{A}^2|A_{\mathrm{gw}} = 0)$ can be described by a Gaussian distribution with zero mean and variance given by $\sigma_0^2$ [Eq. (52)], thus the probability $p(\hat{A}^2 > \hat{A}^2_{\mathrm{thresh}}|A_{\mathrm{gw}} = 0)$ can be expressed in terms of standard deviations away from the mean. For example, if the $\hat{A}^2$ that we measure is 3 standard deviations (i.e $3\sigma$) away from the mean (0 in this case) then this corresponds to a FAP of ∼0.003 meaning that we can rule out the null hypothesis with ∼99.7% confidence. Returning to Eq. (53) we see that the typical frequentist detection procedure mentioned above is contained in this definition of SNR. If we measure a SNR of 3, this carries the same meaning as the FAP above.

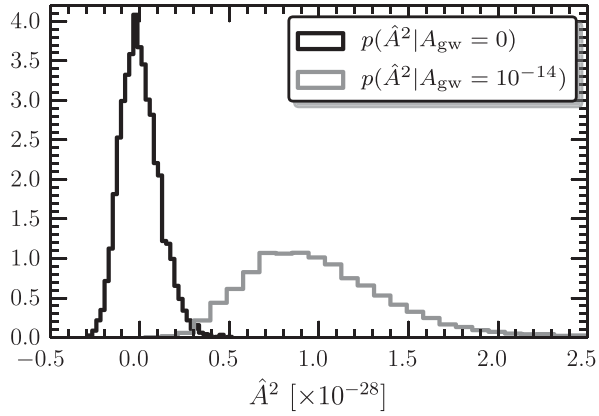


FIG. 2. Histogram of the optimal statistic Eq. (49) in $10^4$ simulations for a PTA consisting of $M = 36$ pulsars, all with rms's $\sigma = 100$ ns, an observational time $T = 5$ years, and a cadence $c = 20\ \mathrm{yr}^{-1}$. We show the distribution of the statistic in the absence of a signal (black line), and the distribution in the presence of a signal with amplitude $A_{\mathrm{gw}} = 10^{-14}$ (gray line). The standard deviation of the distribution in the absence of a signal is $\sigma_0 = 1.08 \times 10^{-29}$.

Figure 2 shows a histogram of the optimal statistic Eq. (49) in $10^4$ simulations for PTA observations of $M = 36$ pulsars, with root-mean-squares (rms's) $\sigma = 100$ ns, for an observational time $T = 5$ years, and a cadence $c = 20\ \mathrm{yr}^{-1}$. The black line shows the distribution of the statistic in the absence of a signal, and the gray curve shows the distribution in the presence of a signal with amplitude $A_{\mathrm{gw}} = 10^{-14}$ (using the methods described below in Sec. IV). The standard deviation of the distribution in the absence of a signal is $\sigma_0 = 1.08 \times 10^{-29}$. As shown in the figure, in the absence of a signal the distribution is not quite Gaussian, but using the true cumulative distribution of the simulations and the $3\sigma$ Gaussian distribution threshold gives a FAP of ∼0.006.

The optimal statistic in Eq. (49) has also been used to analyze the data sets produced for the International PTA Mock Data Challenge. In this challenge, the optimal statistic was used to produce amplitude estimates for three closed data sets. These amplitudes were then compared to those from a first-order likelihood method (described in [40]). The amplitudes recovered using the optimal statistic were consistent with the first-order likelihood methods at the 95% level or better. Readers are encouraged to consult [68] for more details regarding the Mock Data Challenge and the results obtained using the optimal statistic.

## IV. SIMULATED SIGNALS

In this section we describe a software injection procedure that can be used to produce simulated stochastic background signals in PTA data. As we have shown, if a stochastic gravitational-wave background is present, the cross-correlation of timing residuals is given by

$$\langle \tilde{r}_I^*(f)\tilde{r}_J(f')\rangle = \frac{H_0^2}{16\pi^4}\delta(f-f')|f|^{-5}\Omega_{\rm gw}(f)\chi_{IJ}. \quad (56)$$

In the frequency domain it is possible to express the timing residuals as

$$r_I(f) = c(f)\sum_J H_{IJ}w_J(f), \quad (57)$$

where $w_I(f) = x_I(f) + iy_I(f)$ is a complex zero-mean white-noise process, $c(f)$ is a real function that contains information about the spectral index and amplitude of the gravitational-wave spectrum (but does not depend on the pulsar pair), and $H_{IJ}$ is a matrix that linearly combines the timing residuals in such a way as to simulate the expected spatial correlations in the signal, i.e. the Hellings and Downs coefficients.

If the processes $x_I$ and $y_I$ are zero-mean unit-variance processes $w_I(f)$ satisfies

$$\langle w_I^*(f)w_J(f')\rangle = \frac{2}{T}\delta(f-f')\delta_{IJ}, \quad (58)$$

where $T$ is the length of observations, and we can use Eq. (56) to find $c(f)$ and $H_{IJ}$. Taking the ensemble average of Eq. (57) it is easy to show that

$$\langle \tilde{r}_I^*(f)\tilde{r}_J(f')\rangle = \frac{2}{T}c(f)c(f')H_{IJ}H_{JI}\delta(f-f'), \quad (59)$$

which implies that

$$c^2(f)H_{IJ}H_{JI} = \frac{TH_0^2}{32\pi^4}|f|^{-5}\Omega_{\rm gw}(f)\chi_{IJ}. \quad (60)$$

In matrix notation the equation above can be written as

$$c^2(f)\mathbf{H}\mathbf{H}^{\mathbf{T}} = \frac{TH_0^2}{32\pi^4}|f|^{-5}\Omega_{\rm gw}(f)\boldsymbol{\chi}. \quad (61)$$

Relating the functions of frequency on either side of Eq. (61), we readily identify the function $c(f)$ to be

$$c(f) = \left[\frac{TH_0^2}{32\pi^4}\Omega_{\rm gw}(f)|f|^{-5}\right]^{1/2}, \quad (62)$$

along with a condition for the matrix $\mathbf{H}$,

$$\mathbf{H}\mathbf{H}^{\mathbf{T}} = \boldsymbol{\chi} \quad (63)$$

which allows us to determine $\mathbf{H}$ given $\boldsymbol{\chi}$ via a Cholesky decomposition.

To construct simulated timing residuals one can (1) start with $M$ random complex frequency series $w_I(f)$, where $M$ is the number of pulsars, (2) multiply these by $c(f)$, (3) find the Hellings and Downs coefficients for all pulsar pairs and construct the matrix $\boldsymbol{\chi}$, (4) perform a Cholesky decomposition of $\boldsymbol{\chi}$ to find $\mathbf{H}$, and (5) linearly combine the frequency series via Eq. (57) to find $r_I(f)$ for each pulsar. Finally, after inverse Fourier transforming the gravitational-wave residuals, they can be added to real or simulated TOA data that contain additional uncorrelated white- and red-noise components.

## V. SCALING LAWS FOR THE OPTIMAL CROSS-CORRELATION STATISTIC

In [62] the authors considered a simple scenario where pulsar timing residuals have just two noise components, a gravitational-wave red-noise piece and a white-noise piece, which are the same for all pulsars in the PTA, namely

$$\mathcal{P}_I(f) = \mathcal{P}_g(f) + 2\sigma^2\Delta t = bf^{-\gamma} + 2\sigma^2\Delta t. \quad (64)$$

Here all the frequency-independent constants in Eq. (35) have been absorbed into the amplitude $b$, the index $\gamma = 3-2\alpha$ (recall that we are using one-sided power spectra in this paper, in contrast to [62]), and the white-noise rms is denoted by $\sigma$.

In [62] it was shown that the SNR of the optimal cross-correlation scales in three different ways depending on the relative sizes of the gravitational-wave and white-noise components. Specifically the authors found scaling laws for the SNR in

(i) a weak-signal regime where the white-noise component of Eq. (64) is larger than the gravitational-wave piece ($2\sigma_I^2\Delta t \gg bf^{-\gamma}$ at all relevant frequencies),
(ii) the opposite strong signal limit, where $2\sigma_I^2\Delta t \ll bf^{-\gamma}$ at all relevant frequencies, which turns out to be irrelevant for pulsar timing experiments, and
(iii) an intermediate regime between the two cases where the gravitational-wave power spectrum dominates at low frequencies, and the white-noise dominates at high frequencies.

Additionally, they found that the latter regime is likely already relevant to current pulsar timing experiments. In this section we will review the scaling laws for the optimal statistic, and introduce an improved derivation of the scaling law for the intermediate regime.

To derive the scaling laws we begin with the expression for the expected SNR of the cross-correlation statistic,

$$\langle\rho\rangle = A_{\rm gw}^2\left(\sum_{IJ}{\rm tr}[\mathbf{P}_I^{-1}\tilde{\mathbf{S}}_{IJ}\mathbf{P}_J^{-1}\tilde{\mathbf{S}}_{JI}]\right)^{1/2}, \quad (65)$$

which can be written in the frequency domain as [31]

$$\langle\rho\rangle = \left(2T\sum_{IJ}\chi_{IJ}^2\int_{f_L}^{f_H}df\frac{\mathcal{P}_g^2(f)}{\mathcal{P}_I(f)\mathcal{P}_J(f)}\right)^{1/2}. \quad (66)$$

Since we are assuming that all pulsars have the same noise characteristics we can write

$$\langle\rho\rangle = \left(\sum_{IJ}\chi^2_{IJ}\right)^{1/2}\left(2T\int_{f_L}^{f_H} df\,\frac{b^2 f^{-2\gamma}}{(bf^{-\gamma}+2\sigma^2\Delta t)^2}\right)^{1/2}. \tag{67}$$

In the weak-signal regime, where $2\sigma_I^2\Delta t \gg bf^{-\gamma}$ for all frequencies of interest, i.e., $f\in[f_L,f_H]$, the SNR is well approximated by

$$\langle\rho\rangle \approx \left(\sum_{IJ}\chi^2_{IJ}\right)^{1/2}\frac{bcT^\gamma}{2\sigma^2\sqrt{\gamma-1/2}}, \tag{68}$$

where $c=1/\Delta t$ is the cadence.

In the intermediate regime we cannot use this approximation because at low frequencies the power in the gravitational-wave background is larger than the white-noise level. Note that this happens when $bT^\gamma > 2\sigma^2\Delta t$, and the condition on the white-noise rms is

$$\sigma < \frac{A}{\pi f^\alpha_{1\ \mathrm{yr}}}\sqrt{\frac{cT^\gamma}{24}}. \tag{69}$$

For pulsar timing experiment durations of $T=5$ yr, cadence of $c=20\ \mathrm{yr}^{-1}$, for a background with amplitude $A=10^{-15}$, and a spectral index like the one we expect for the SMBBH background ($\gamma=13/3$), the pulsar timing array is in the weak-signal limit only if the pulsars have white-noise rms's greater than about 300 ns. There are already a handful of pulsars that are currently timed with better precisions than that (see, for example, [37]).

In this case the integral in Eq. (67) must be evaluated generally. To do this, we write the integral as

$$\int_{f_L}^{f_H} df F(f) = \int_0^{f_H} df F(f) - \int_0^{f_L} df F(f) \tag{70}$$

where for convenience we have written

$$F(f) = \frac{bf^{-2\gamma}}{(bf^{-\gamma}+2\sigma^2\Delta t)^2}. \tag{71}$$

The integrals on the right-hand side of Eq. (70) have analytic solutions in terms of ordinary hypergeometric functions. To proceed, we evaluate the integral of $F(f)$ over a generic interval $[0,f_*]$ which yields

$$\int_0^{f_*} df F(f) = \frac{f_*}{\gamma}\left[\frac{1}{1+\frac{2\sigma^2\Delta t}{bf_*^{-\gamma}}}+(\gamma-1)G\left(\frac{-2\sigma^2\Delta t}{bf_*^{-\gamma}}\right)\right], \tag{72}$$

where $G(x) = {}_2F_1(1,\gamma^{-1},1+\gamma^{-1},x)$. We can probe this solution in the context of Eq. (70) by replacing $f_*$ with $f_H$ or $f_L$.

For the second integral on the right-hand side of Eq. (70) where $f_* = f_L = 1/T$, we have $(2\sigma^2\Delta t)/(bf_L^{-\gamma}) \ll 1$ and the hypergeometric function can be approximated to be unity

$${}_2F_1\left(1,\gamma^{-1},1+\gamma^{-1},\frac{-2\sigma^2\Delta t}{bf_L^{-\gamma}}\right)\approx 1.$$

This simplifies Eq. (72) greatly, and the integral is easily evaluated as

$$\int_0^{f_L} df F(f) \approx \frac{1}{T}. \tag{73}$$

To evaluate the first integral in Eq. (70), we consider the case when $f_* = f_H$ in Eq. (72). In this case, since $(2\sigma^2\Delta t)/(bf_H^{-\gamma}) \gg 1$, the integral can be approximated as

$$\int_0^{f_H} df F(f) \approx \frac{f_H}{\gamma}\left[\frac{bf_H^{-\gamma}}{2\sigma^2\Delta t}+(\gamma-1)G\left(\frac{-2\sigma^2\Delta t}{bf_H^{-\gamma}}\right)\right]. \tag{74}$$

We can then use standard identities relating the hypergeometric function to inverses of their arguments [see, for example, Eq. (15.8.2) in [68]]. Using these identities along with Euler's reflection formula we obtain

$$\begin{aligned}\int_0^{f_H} df F(f) \approx \frac{f_H}{\gamma}\Bigg\{&\frac{bf_H^{-\gamma}}{2\sigma^2\Delta t}+(\gamma-1)\Gamma(\gamma^{-1}-1)\Gamma(2-\gamma^{-1})\Gamma(1+\gamma^{-1})\\ &\times\left[\frac{bf_H^{-\gamma}}{2\sigma^2\Delta t}\frac{\Gamma(2-\gamma^{-1})^{-1}}{\Gamma(\gamma^{-1})^2}{}_2F_1\left(1,1-\gamma^{-1},2-\gamma^{-1};\frac{-bf_H^{-\gamma}}{2\sigma^2\Delta t}\right)-\frac{1}{\Gamma(\gamma^{-1})}\left(\frac{bf_H^{-\gamma}}{2\sigma^2\Delta t}\right)^{1/\gamma}{}_2F_1\left(\gamma^{-1},0,\gamma^{-1};\frac{-bf_H^{-\gamma}}{2\sigma^2\Delta t}\right)\right]\Bigg\}.\end{aligned} \tag{75}$$

Since $bf_H^{-\gamma}/2\sigma^2\Delta t \ll 1$ both hypergeometric functions can be well approximated by unity. Additionally, since $bf_H^{-\gamma}/2\sigma^2\Delta t \ll (bf_H^{-\gamma}/2\sigma^2\Delta t)^{1/\gamma}$ for $\gamma>1$, the last term in Eq. (75) dominates and the expression can be simplified to

$$\int_0^{f_H} df F(f) \approx \kappa(\gamma)\left(\frac{b}{2\sigma^2\Delta t}\right)^{1/\gamma} \tag{76}$$

with

$$\kappa(\gamma) = \frac{(1-\gamma)\Gamma(\gamma^{-1}-1)\Gamma(2-\gamma^{-1})\Gamma(1+\gamma^{-1})}{\gamma\Gamma(\gamma^{-1})}. \quad (77)$$

Putting the results of Eqs. (73) and (76) together, we arrive at the solution to the original problem posed in Eq. (70):

$$\int_{f_L}^{f_H} df F(f) \approx \kappa(\gamma)\left(\frac{b}{2\sigma^2\Delta t}\right)^{(1/\gamma)} - \frac{1}{T}. \quad (78)$$

In terms of the cadence $c = 1/\Delta t$ the average value of the SNR is therefore given by

$$\langle\rho\rangle \approx \left(\sum\nolimits_{IJ}\chi^2_{IJ}\right)^{1/2}\left[2T\left(\kappa(\gamma)\left(\frac{bc}{2\sigma^2}\right)^{(1/\gamma)} - \frac{1}{T}\right)\right]^{1/2}. \quad (79)$$

At late times,

$$\langle\rho\rangle \approx \left(\sum\nolimits_{IJ}\chi^2_{IJ}\right)^{1/2}\left[2T\kappa(\gamma)\left(\frac{bc}{2\sigma^2}\right)^{(1/\gamma)}\right]^{1/2} \propto M\left(\frac{cA^2_{\rm gw}}{2\sigma^2}\right)^{1/(2\gamma)} T^{1/2}. \quad (80)$$

In [62] the authors approximated the integral in a less accurate (albeit more pedagogical) way: they found the frequency $f_r = (bc/2\sigma^2)^{1/\gamma}$ at which the gravitational-wave red noise equals the white noise, and assumed the integral was gravitational-wave dominated at frequencies lower than $f_r$, and white-noise dominated at frequencies higher than $f_r$. The integrals then become trivial. The result is the same as Eq. (79), but with a different value of the coefficient $\kappa$ which was found to be $\kappa' = 2\gamma/(2\gamma-1)$. In the approximation the integrand for the SNR is always overestimated and the value of $\kappa'$ is larger than what we have calculated for $\kappa$ in this paper.

Figure 3 shows the average SNR versus time in years for PTA with 20 pulsars timed with a precision of $\sigma =$ 50 ns and a gravitational-wave background produced by SMBBHs ($\gamma = 13/3$) with an amplitude $A_{\rm gw} = 10^{-15}$. The gray curve shows the SNR computed numerically in the time domain using Eq. (65). For the timing model we have subtracted out a quadratic—i.e., we have fitted out a quadratic with the **R** projection matrices in the time domain. The dotted curve shows the average SNR as computed in the weak-signal limit using Eq. (68). The dashed-dot curve shows the SNR in the intermediate regime at late times as calculated using Eq. (80). Finally, the dashed curve shows the SNR calculated using Eq. (79). At very early times the approximation is not valid: the first term in the square root is smaller than $1/T$ so the SNR is imaginary. At later times the predicted SNR is in excellent agreement with the time-domain numerical calculation. Note the remarkable accuracy with which the low-frequency cutoff $f_L = 1/T$ approximates the effect of quadratic subtraction.

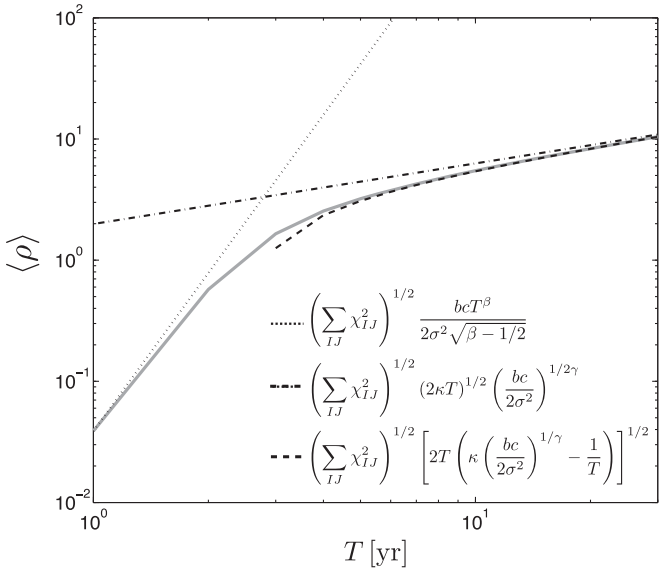


FIG. 3. Average SNR versus time in years for PTA with 20 pulsars timed with a precision of $\sigma = 50$ ns and a gravitational-wave background produced by SMBBHs ($\gamma = 13/3$) with an amplitude $A_{\rm gw} = 10^{-15}$. The gray curve shows the SNR computed numerically using Eq. (65). The dotted curve shows SNR in the weak-signal limit, Eq. (68). The dashed-dot curve shows the SNR in the intermediate regime at late times, Eq. (80). The dashed curve shows the SNR calculated using Eq. (79).

## VI. SUMMARY

In this paper, we have presented a time-domain implementation of the optimal cross-correlation statistic for stochastic gravitational-wave background searches using PTA data, originally presented in [31]. The derivation and implementation described here extends that of [31] by taking the timing model into account in a natural and statistically well-motivated way by including the linear timing model directly into the likelihood function, allowing for analytic maximization of the timing model parameters. The time-domain implementation also allows one to fully model the noise and naturally deal with nonstationarities and irregular sampling of the data, which cannot be modeled in the frequency domain.

An alternative approach for analyzing PTA data for stochastic gravitational-wave backgrounds is to use Bayesian inference, as described in [33,35,40,69,70]. In the Bayesian approach, one constructs the posterior probability distributions for the noise and gravitational-wave signal parameters via Bayes's theorem by specifying the likelihood function for the data given a set of model gravitational-wave and noise parameters and a prior distribution on the model parameters. By marginalizing over

the model parameters, one also constructs the Bayesian evidence for various models, which allow for the construction of Bayes factors (ratio of Bayesian evidence) to determine which model is favored by the data.

While we believe that a Bayesian approach to the detection problem for stochastic backgrounds is preferred and indeed recommended, the frequentist cross-correlation statistic presented here has several advantages over the Bayesian approach. First, the optimal statistic approach is computationally inexpensive as it involves only a single function call (given a set of modeled noise parameters), while the Bayesian method must explore a very large-dimensional space leading to millions of likelihood evaluations. For current data sets, the optimal statistic can be evaluated in seconds while the full Bayesian approach can take weeks to run on a supercomputer.

Furthermore, the SNR as defined in this work is a good approximation to the Bayes factor comparing a model for a correlated gravitational-wave background to a model for an uncorrelated intrinsic red-noise source. Thus the computationally inexpensive optimal statistic has proven invaluable in large-scale simulations and projections of detector sensitivity as it allows us to test many different signal models and pulsar observation scenarios with relative ease, while full Bayesian simulations on this scale are unfeasible. In addition, the relationship between the optimal statistic SNR and the Bayes factors affords an analytically tractable environment from which to construct various scaling relations as shown in Fig. 3.

The optimal statistic does have two major drawbacks that make it less desirable as a production-level detection statistic compared to the Bayes factor. First, the point estimate of the amplitude of the gravitational-wave background depends on our ability to accurately model the total autocorrelated power for each pulsar. Typically this is done by modeling the noise for each pulsar *independently* and then including the maximum likelihood values in the autocovariance matrices of the optimal statistic. If the signal is loud and the data do not contain any intrinsic red noise then this method is fairly robust and does not significantly bias results. However, if the signal is weak or there is other intrinsic red noise then this method will lead to biases. In low SNR scenarios the red noise due to the stochastic background may not be large enough to detect in an individual pulsar and will thus not enter the autocovariance matrices used in the optimal statistic. This will lead to an inconsistency in the optimal statistic where it will still be able to detect cross-correlated power, but the point estimate of the amplitude will be biased low because the autocovariance terms (from our single pulsar noise analysis) indicate that the red noise is very weak.

This problem does not arise in Bayesian analyses because the intrinsic pulsar noise and the stochastic background parameters are modeled *simultaneously.* This problem could be ameliorated by performing the initial noise modeling over all pulsars simultaneously and including a correlated gravitational-wave background component. These noise estimates (which will include a common gravitational-wave background term in the autocovariance) could then be input to the optimal statistic.

Despite these drawbacks, the optimal cross-correlation statistic serves as a proxy for a full Bayesian search when performing computationally intensive simulations and will also serve as a very useful cross-check when making detection statements on future PTA data.

## ACKNOWLEDGMENTS

We thank Eanna Flanagan for pointing out a sign error in [31], which has been corrected here. We also thank Chris Pankow and Madeline Wade for many useful comments and suggestions. We extend our gratitude to the members of the NANOGrav Data Analysis Working Group. The work of S. J. C., X. S., and J. A. E. was partially funded by the National Science Foundation (NSF) through CAREER Grant No. 0955929, Partnerships for International Research and Education (PIRE) Grant No. 0968126, Grant No. 0970074, and the Wisconsin Space Grant Consortium. J. A. E. acknowledges support by National Aeronautics and Space Administration (NASA) through Einstein Fellowship Grant No. PF4-150120. J. D. R. would like to acknowledge support from NSF Gants No. HRD-0734800, No. HRD-1242090, and No. PHY-1205585.

## APPENDIX: RELATION TO DEMOREST *et al.* CROSS-CORRELATION STATISTIC

Here we show that the optimal statistic, although derived in a different manner, is identical to the cross-correlation statistic presented in [37]. In the notation used in this work, the cross-correlation coefficients can be written as

$$\rho_{IJ} = \frac{\mathbf{r}_I^T \mathbf{P}_I^{-1} \hat{\mathbf{S}}_{IJ} \mathbf{P}_J^{-1} \mathbf{r}_J}{\mathrm{tr}[\mathbf{P}_I^{-1} \hat{\mathbf{S}}_{IJ} \mathbf{P}_J^{-1} \hat{\mathbf{S}}_{JI}]}, \tag{A1}$$

where $\hat{\mathbf{S}}_{IJ}$ is defined so that $A_{\mathrm{gw}}^2 \chi_{IJ} \hat{\mathbf{S}}_{IJ} = \mathbf{S}_{IJ}$. The uncertainty on the correlation coefficients is

$$\sigma_{IJ} = (\mathrm{tr}[\mathbf{P}_I^{-1} \hat{\mathbf{S}}_{IJ} \mathbf{P}_J^{-1} \hat{\mathbf{S}}_{JI}])^{-1/2}. \tag{A2}$$

With these expressions we now have an estimate of the cross-correlation coefficients along with their uncertainty for each pulsar pair. Notice that only the spectral shape of the gravitational-wave background is assumed. To determine an estimate of the gravitational-wave background amplitude, the following chi squared is minimized

$$\chi^2 = \sum_{IJ} \left( \frac{\rho_{IJ} - A_{\mathrm{gw}}^2 \chi_{IJ}^2}{\sigma_{IJ}} \right)^2. \tag{A3}$$

The resulting best fit gravitational-wave amplitude is

$$\hat{A}^2_{\rm gw} = \sum_{IJ} \frac{\rho_{IJ}\chi_{IJ}}{\sigma^2_{IJ}} \Big/ \sum_{IJ} \frac{\chi^2_{IJ}}{\sigma^2_{IJ}}, \tag{A4}$$

with variance

$$\sigma^2 = \left( \sum\nolimits_{IJ} \frac{\chi^2_{IJ}}{\sigma^2_{IJ}} \right)^{-1}. \tag{A5}$$

By using Eqs. (A1) and (A2) and by noting that $\chi_{IJ}\hat{\mathbf{S}}_{IJ} = \tilde{\mathbf{S}}_{IJ}$, we obtain

$$\hat{A}^2_{\rm gw} = \frac{\sum_{IJ} \mathbf{r}_I^T \mathbf{P}_I^{-1} \tilde{\mathbf{S}}_{IJ} \mathbf{P}_J^{-1} \mathbf{r}_J}{\sum_{IJ} \mathrm{tr}[\mathbf{P}_I^{-1} \tilde{\mathbf{S}}_{IJ} \mathbf{P}_J^{-1} \tilde{\mathbf{S}}_{JI}]}, \tag{A6}$$

which is identical to Eq. (49).


[1] G. Hobbs *et al.*, Classical Quantum Gravity **27**, 084013 (2010).
[2] R. A. Hulse and J. H. Taylor, Astrophys. J. Lett. **195**, L51 (1975).
[3] M. V. Sazhin, Sov. Astron. **22**, 36 (1978).
[4] S. Detweiler, Astrophys. J. **234**, 1100 (1979).
[5] A. H. Jaffe and D. C. Backer, Astrophys. J. **583**, 616 (2003).
[6] A. Sesana, A. Vecchio, and C. N. Colacino, Mon. Not. R. Astron. Soc. **390**, 192 (2008).
[7] A. Sesana, A. Vecchio, and M. Volonteri, Mon. Not. R. Astron. Soc. **394**, 2255 (2009).
[8] A. N. Lommen and D. C. Backer, Astrophys. J. **562**, 297 (2001).
[9] J. S. B. Wyithe and A. Loeb, Astrophys. J. **590**, 691 (2003).
[10] M. Volonteri, F. Haardt, and P. Madau, Astrophys. J. **582**, 559 (2003).
[11] M. Enoki, K. T. Inoue, M. Nagashima, and N. Sugiyama, Astrophys. J. **615**, 19 (2004).
[12] A. Sesana, Mon. Not. R. Astron. Soc. **433**, L1 (2013).
[13] S. T. McWilliams, J. P. Ostriker, and F. Pretorius, arXiv: 1211.4590.
[14] A. Sesana and A. Vecchio, Phys. Rev. D **81**, 104008 (2010).
[15] C. Roedig and A. Sesana, J. Phys. Conf. Ser. **363**, 012035 (2012).
[16] V. Ravi, J. S. B. Wyithe, G. Hobbs, R. M. Shannon, R. N. Manchester, D. R. B. Yardley, and M. J. Keith, Astrophys. J. **761**, 84 (2012).
[17] C. M. F. Mingarelli, K. Grover, T. Sidery, R. J. E. Smith, and A. Vecchio, Phys. Rev. Lett. **109**, 081104 (2012).
[18] R. van Haasteren and Y. Levin, Mon. Not. R. Astron. Soc. **401**, 2372 (2010).
[19] J. Cordes and F. Jenet, Astrophys. J. **752**, 54 (2012).
[20] S. Olmez, V. Mandic, and X. Siemens, Phys. Rev. D **81**, 104028 (2010).
[21] L. Sousa and P. P. Avelino, Phys. Rev. D **88**, 023516 (2013).
[22] K. Miyamoto and K. Nakayama, J. Cosmol. Astropart. Phys. 7 (2013) 012.
[23] S. Kuroyanagi, K. Miyamoto, T. Sekiguchi, K. Takahashi, and J. Silk, Phys. Rev. D **87**, 023522 (2013).
[24] C. Caprini, R. Durrer, and X. Siemens, Phys. Rev. D **82**, 063511 (2010).
[25] A. A. Starobinsky, JETP Lett. **30**, 682 (1979).
[26] W. Zhao, Y. Zhang, X.-P. You, and Z.-H. Zhu, Phys. Rev. D **87**, 124012 (2013).
[27] D. R. Stinebring, M. F. Ryba, J. H. Taylor, and R. W. Romani, Phys. Rev. Lett. **65**, 285 (1990).
[28] A. N. Lommen, arXiv:astro-ph/0208572.
[29] F. A. Jenet, G. B. Hobbs, K. J. Lee, and R. N. Manchester, Astrophys. J. Lett. **625**, L123 (2005).
[30] F. A. Jenet, G. B. Hobbs, W. van Straten, R. N. Manchester, M. Bailes, J. P. W. Verbiest, R. T. Edwards, A. W. Hotan, J. M. Sarkissian, and S. M. Ord, Astrophys. J. **653**, 1571 (2006).
[31] M. Anholm, S. Ballmer, J. D. E. Creighton, L. R. Price, and X. Siemens, Phys. Rev. D **79**, 084030 (2009).
[32] R. van Haasteren, Y. Levin, P. McDonald, and T. Lu, Mon. Not. R. Astron. Soc. **395**, 1005 (2009).
[33] R. van Haasteren, Y. Levin, P. McDonald, and T. Lu, Mon. Not. R. Astron. Soc. **395**, 1005 (2009).
[34] D. R. B. Yardley *et al.*, Mon. Not. R. Astron. Soc. **414**, 1777 (2011).
[35] R. van Haasteren *et al.*, Mon. Not. R. Astron. Soc. **414**, 3117 (2011).
[36] J. M. Cordes and R. M. Shannon, Astrophys. J. **750**, 89 (2012).
[37] P. B. Demorest *et al.*, Astrophys. J. **762**, 94 (2013).
[38] L. Boyle and U.-L. Pen, Phys. Rev. D **86**, 124028 (2012).
[39] R. van Haasteren and Y. Levin, Mon. Not. R. Astron. Soc. **428**, 1147 (2013).
[40] J. Ellis, X. Siemens, and R. van Haasteren, Astrophys. J. **769**, 63 (2013).
[41] C. M. F. Mingarelli, T. Sidery, I. Mandel, and A. Vecchio, Phys. Rev. D **88**, 062005 (2013).
[42] S. R. Taylor and J. R. Gair, Phys. Rev. D **88**, 084001 (2013).
[43] J. Gair, J. D. Romano, S. Taylor, and C. M. F. Mingarelli, Phys. Rev. D **90**, 082001 (2014).
[44] C. M. F. Mingarelli and T. Sidery, Phys. Rev. D **90**, 062011 (2014).
[45] J. A. Ellis, X. Siemens, and J. D. E. Creighton, Astrophys. J. **756**, 175 (2012).
[46] A. Petiteau, S. Babak, A. Sesana, and M. de Araújo, Phys. Rev. D **87**, 064036 (2013).
[47] J. A. Ellis, F. A. Jenet, and M. A. McLaughlin, Astrophys. J. **753**, 96 (2012).

[48] M.-L. Tong, B.-R. Yan, C.-S. Zhao, D.-S. Yin, S.-H. Zhao, T.-G. Yang, and Yu-P. Gao, Chin. Phys. Lett. **30**, 100402 (2013).
[49] S. Taylor, J. Ellis, and J. Gair, Phys. Rev. D **90**, 104028 (2014).
[50] Z. Arzoumanian *et al.*, Astrophys. J. **794**, 141 (2014).
[51] Y. Wang, S. D. Mohanty, and F. A. Jenet, Astrophys. J. **795**, 96 (2014).
[52] S. Yi, B. W. Stappers, S. A. Sanidas, C. G. Bassa, G. H. Janssen, A. G. Lyne, M. Kramer, and S.-N. Zhang, Mon. Not. R. Astron. Soc. **445**, 1245 (2014).
[53] X.-J. Zhu *et al.*, Mon. Not. R. Astron. Soc. **444**, 3709 (2014).
[54] L. S. Finn and A. N. Lommen, Astrophys. J. **718**, 1400 (2010).
[55] J. Cordes and F. Jenet, Astrophys. J. **752**, 54 (2012).
[56] M. Pitkin, Mon. Not. R. Astron. Soc. **425**, 2688 (2012).
[57] D. R. Madison, J. M. Cordes, and S. Chatterjee, Astrophys. J. **788**, 141 (2014).
[58] X. Deng, Phys. Rev. D **90**, 024020 (2014).
[59] C. Cutler, S. Burke-Spolaor, M. Vallisneri, J. Lazio, and W. Majid, Phys. Rev. D **89**, 042003 (2014).
[60] B. Allen and J. D. Romano, Phys. Rev. D **59**, 102001 (1999).
[61] R. W. Hellings and G. S. Downs, Astrophys. J. Lett. **265**, L39 (1983).
[62] X. Siemens, J. Ellis, F. Jenet, and J. D. Romano, Classical Quantum Gravity **30**, 224015 (2013).
[63] W. H. Press, S. A. Teukolsky, W. T. Vetterling, and B. P. Flannery, *Numerical Recipes in C: The Art of Scientific Computing*, 2nd ed. (Cambridge University Press, New York, USA, 1992).
[64] P. B. Demorest, Ph.D. thesis, University of California, Berkeley, 2007.
[65] G. B. Hobbs, R. T. Edwards, and R. N. Manchester, Mon. Not. R. Astron. Soc. **369**, 655 (2006).
[66] W. Coles, G. Hobbs, D. J. Champion, R. N. Manchester, and J. P. W. Verbiest, Mon. Not. R. Astron. Soc. **418**, 561 (2011).
[67] J. A. Ellis *et al.* (to be published).
[68] F. W. Olver, D. W. Lozier, R. F. Boisvert, and C. W. Clark, *NIST Handbook of Mathematical Functions*, 1st ed. (Cambridge University Press, New York, USA, 2010).
[69] L. Lentati, P. Alexander, M. P. Hobson, S. Taylor, and S. T. Balan, Phys. Rev. D **87**, 104021 (2013).
[70] S. R. Taylor, J. R. Gair, and L. Lentati, arXiv:1210.3489.